

## Journal Pre-proofs

Hydrogen evolution reaction at lead/carbon porous electrodes studied by a novel electrochemical mass spectrometry set-up

Tomás M. Mondino, Gonzalo García, Elena Pastor, Fernando Fungo, Gabriel A. Planes

PII: S1388-2481(22)00195-3  
DOI: <https://doi.org/10.1016/j.elecom.2022.107393>  
Reference: ELECOM 107393

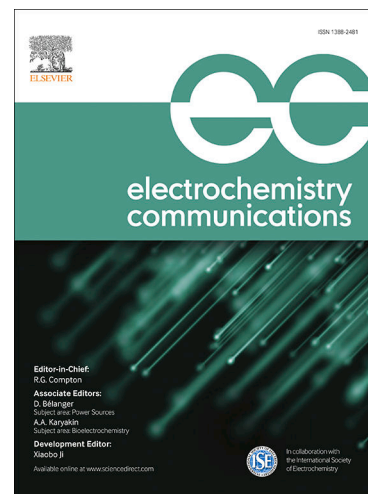
To appear in: *Electrochemistry Communications*

Received Date: 19 October 2022  
Revised Date: 4 November 2022  
Accepted Date: 8 November 2022

Please cite this article as: T.M. Mondino, G. García, E. Pastor, F. Fungo, G.A. Planes, Hydrogen evolution reaction at lead/carbon porous electrodes studied by a novel electrochemical mass spectrometry set-up, *Electrochemistry Communications* (2022), doi: <https://doi.org/10.1016/j.elecom.2022.107393>

This is a PDF file of an article that has undergone enhancements after acceptance, such as the addition of a cover page and metadata, and formatting for readability, but it is not yet the definitive version of record. This version will undergo additional copyediting, typesetting and review before it is published in its final form, but we are providing this version to give early visibility of the article. Please note that, during the production process, errors may be discovered which could affect the content, and all legal disclaimers that apply to the journal pertain.

© 2022 Published by Elsevier B.V.





## 25 **Abstract**

26 Lead–acid batteries are robust, low-cost, and have a large power-to-weight ratio. Recently,  
27 small amounts of carbon-based materials with a high surface area have been included in the  
28 Pb electrode as additives to improve the high-rate partial state of charge. However, carbon-  
29 based materials also enhance the hydrogen evolution reaction during the charging process at  
30 the negative active material (NAM), which is undesirable and dangerous. Therefore, in the  
31 current communication, a promising differential electrochemical mass spectrometry (DEMS)  
32 set-up suitable for studying the hydrogen evolution reaction (HER) at technical NAM  
33 electrodes in lead–acid batteries (LABs) is reported for the first time.

34

## 35 **1- Introduction**

36 Lead–acid batteries (LABs) were proposed by Gaston Planté in 1860 and the first  
37 report published 19 years later [1]. This was the first practical rechargeable battery and is  
38 now more than 150 years old. The formidable strength of lead–acid technology allowed it to  
39 survive for this length of time without significant changes to the central concept [2]. In this  
40 century, carbon-based materials with a high surface area have been employed to enhance the  
41 performance of lead–acid batteries [3].

42 The main challenge of LABs is to improve the high-rate partial-state-of-charge (HRPSoC)  
43 performance, which is important in many applications. There is strong evidence of the benefit  
44 of introducing small amounts (ca. 1–2 % w/w) of a carbon-based material with a high surface  
45 area as an additive into the lead–acid anode (Pb/C, usually called the negative active material  
46 or ‘NAM’) [4,5]. This inhibits sulfation and increases the capacitance and therefore the  
47 charge acceptance of the batteries [36].

48 However, the insertion of carbon-based materials into the NAM may also enhance the  
49 hydrogen evolution reaction (HER) during the charging process, which strongly affects the  
50 battery life cycle [3,711]. Therefore, current research is focused on the development of new  
51 materials that increase the capacitance while inhibiting sulfation and the HER at lead-based  
52 electrodes [3,12].

53 A number of techniques have been employed to study the HER in LABs, including volume  
54 measurements (VM), electrochemical impedance spectroscopy (EIS), rotating ring-disk  
55 electrode (RRDE), current transients (CTs) and cyclic voltammetry (CV) [1318]. It should  
56 be noted that none of these techniques provide in situ detection and quantification of the HER  
57 at lead-based electrodes. In this context, differential electrochemical mass spectrometry  
58 (DEMS) appears to be a valuable technique capable of performing in situ measurements of  
59 the onset potential of the HER as well as quantifying the amount of hydrogen produced at  
60 lead-based electrodes [1921].

61 In this paper we demonstrate the versatility and high sensitivity of the meniscus-based  
62 approach of a novel on-line DEMS set-up by studying the HER at technical NAM electrodes.  
63 Using this approach, H<sub>2</sub> is accurately detected for the first time on-line at lead-based  
64 electrodes.

65

## 66 **2- Experimental**

### 67 *2.1 Electrochemical characterization*

68 All electrochemical measurements were performed in a conventional three-electrode cell  
69 controlled by a PC Autolab potentiostat-galvanostat PGSTAT30. A reversible hydrogen  
70 electrode (RHE) was used as the reference and an activated carbon cloth as the counter  
71 electrode. All potentials in this work are given against the RHE. Experiments were carried

72 out in 5.0 M aqueous sulfuric solutions prepared from high purity reagents (Merck p.a.) and  
73 ultra-pure water (Millipore MilliQ gradient A10 system, 18.2 M $\Omega$  cm, 2 ppb total organic  
74 carbon). Argon (N50, Air Liquide) was used to deoxygenate all solutions.

75

## 76 *2.2 New DEMS set-up*

77 The electrode configuration used for the new DEMS set-up is shown in **Figure 1**. A small  
78 Pb cylinder with a central hole for a DEMS capillary tube (PTFE, Supelco<sup>®</sup>) was employed  
79 as a conductive holder. The tube is partially inserted into the Pb holder, and the end of the  
80 capillary tube sealed with a porous membrane (PTFE, Gore-Tex<sup>®</sup>) interface. The remaining  
81 space inside the Pb hole is used to hold the sample. DEMS experiments were performed using  
82 a commercial mass spectrometer from Pfeiffer (Omnistar<sup>®</sup>).

83

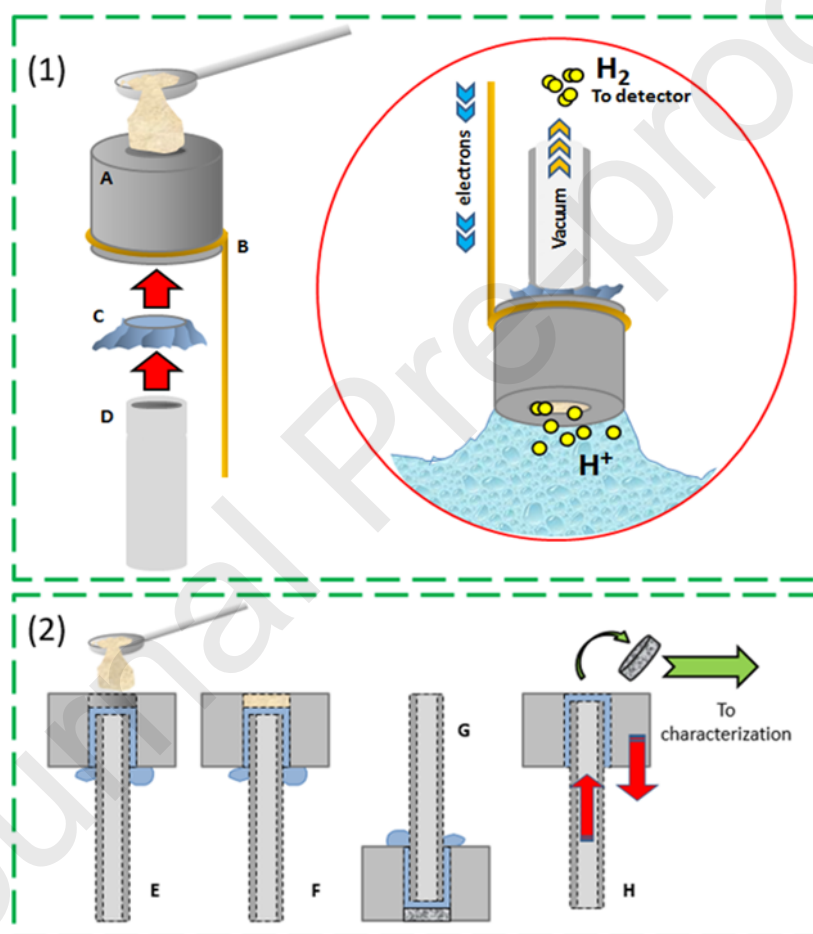
## 84 *2.3 Working electrode preparation*

85 *Carbonaceous material:* Two commercial carbon materials were tested: (i) HE 631 expander  
86 (Hammond<sup>®</sup>), denoted 'HE'; and (ii) SuperP Carbon black (Timcal<sup>®</sup>), denoted 'SP'.

87 *Carbon-based ink:* The suspension was prepared by stirring 20 mg of the carbonaceous  
88 material with 30  $\mu$ L of Nafion<sup>®</sup> (5%, Sigma-Aldrich) and 1.0 mL of water (Milli-Q,  
89 Millipore).

90 *DEMS measurements of technical NAM electrodes:* NAM electrodes were obtained by  
91 electrochemical reduction of an aqueous mixture precursor PbO (Pb, Sigma-Aldrich), PbO +  
92 HE (Pb/HE) or PbO +SP (Pb/SP) (1 wt.% of carbonaceous material) once the NAM mixture  
93 was introduced into the Pb holder (see **Figure 1**). Then, the precursor was exposed for 1 h at  
94 ambient temperature for drying. The electrochemical reduction was carried out by applying  
95 -0.45 V vs RHE until 2.9  $^{\circ}$ C was reached. Finally, the electrode was left in Milli-Q water for

96 48 h, replacing the liquid every 2 h. The final size of the NAM (1 mm thick) is defined by  
 97 the holder diameter and the distance from the surface to the porous membrane ( $\varnothing \approx 1.5$  mm,  
 98 1 mm high). **Figure SI-1** shows representative SEM images of the NAM electrodes obtained  
 99 following the procedure detailed in **Figure 1**. A porous structure with a layer thickness close  
 100 to 1 mm can be observed, which is similar to that of technical (operative) LAB-NAM  
 101 electrodes.



102

103 **Figure 1.** (1) (A) Pb holder, (B) Au wire, (C) PTFE membrane, (D) PTFE capillary; and a scheme  
 104 showing the set-up in operation (right). (2) (E) Loading the NAM precursor (PbO or PbO/C), (F)  
 105 layer formation, (G) electrochemical reduction of the precursor to give NAM (Pb or Pb/C) and  
 106 subsequent electrochemical/DEMS analysis, (H) transfer of the NAM layer for further  
 107 characterization.

108

109 **3- Results and discussion**

110

111 *3.1- HER at NAM electrodes*

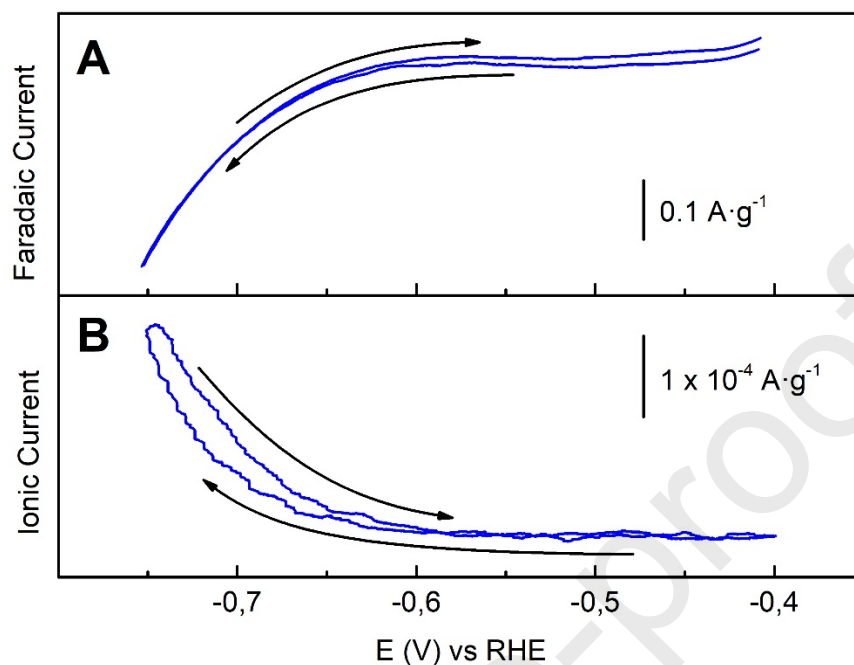
112 DEMS analysis at a NAM surface is quite different from any other system examined by  
113 DEMS to date. A conventional DEMS analysis implies a thin layer porous electrode, which  
114 ensures fast tracking of any volatile species produced at any point of the electrode surface,  
115 with the behavior of current and mass signals followed on-line [20,2224].

116 On the other hand, a real (operative) NAM layer requires a thickness in the order of ~1 mm,  
117 which is quite a lot thicker than the typical electrodes studied by DEMS [19,22,23]. The latter  
118 size is in agreement with the electrodes synthesized in the current work (see **Figure SI-1**).

119 Moreover, **Figure SI-2** reveals that all the electrodes tested in the current work have a  
120 specific capacity close to 100 mAh g<sup>-1</sup>, which is a typical value for a conventional NAM [25].

121 **Figure 2** shows a cyclic voltammogram (CV) and the corresponding mass spectrometry  
122 cyclic voltammogram (MSCV) for the  $m/z = 2$  signal recorded simultaneously at the Pb/SP  
123 electrode with a short delay of ca. 5 s, which should be ascribed to the porous structure and  
124 consequent facile diffusion of species at NAM electrodes [15,22]. It is remarkable that the  
125 ionic currents are on-line with the faradaic ones. Indeed, the MSCV for the  $m/z = 2$  signal  
126 ( $\text{H}_2^+$ ), which is associated with  $\text{H}_2$  formation, accurately reveals the onset potential for the  
127 HER at NAM electrodes.

128



129

130 **Figure 2.** (A) CV and (B) MSCVs ( $m/z = 2$ ) recorded at Pb/SP electrode.  $V = 1 \text{ mV s}^{-1}$ ;  $5 \text{ M H}_2\text{SO}_4$ .131  $T = 25 \text{ }^\circ\text{C}$ .

132

133 **Figure 3** compares linear sweep voltammograms (LSVs) and the corresponding mass linear  
 134 sweep voltammograms (MSLSVs) for the mass signal = 2 recorded at Pb/SP, Pb/HE and Pb  
 135 electrodes. As expected, the introduction of carbon materials into the NAM enhances the  
 136 HER. Indeed, the onset overpotentials for the HER increase as follows: Pb/SP < Pb/HE < Pb.  
 137 On the other hand, **Figure SI-3** reveals that HE has a higher capacitance value ( $6.72 \text{ F g}^{-1}$ )  
 138 than SP ( $1.01 \text{ F g}^{-1}$ ).

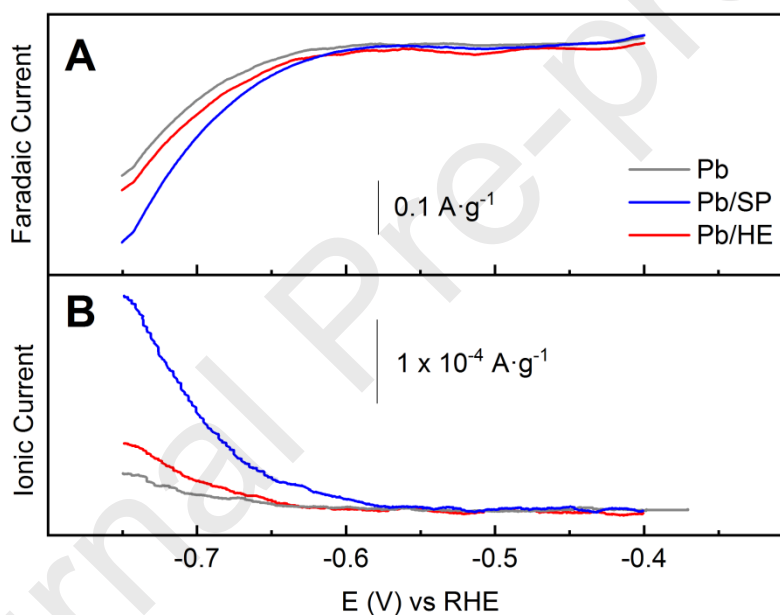
139 Unlike the well-characterized SP carbon, HE carbon is a commercial expander provided  
 140 especially for NAM applications in LABs, and contains several additives such as carbon  
 141 black, lignosulfonate and barium sulfate among others, and therefore it is not possible to  
 142 obtain a full physicochemical characterization of this material. Nevertheless, Figure SI-3 and



143 Figure 3 indicate that the HER contribution of a specific carbon surface is strongly dependent  
 144 on the nature of the carbon.

145 It is important to recall that a high capacitance value and low HER contribution are of  
 146 paramount importance in enhancing the performance of NAM electrodes, i.e. a low-cost  
 147 additive with high surface area, capacitance, electrical conductivity and onset overpotential  
 148 toward the HER is desirable to enhance the performance of NAM electrodes, and therefore  
 149 HE appears to be a promising additive.

150



151

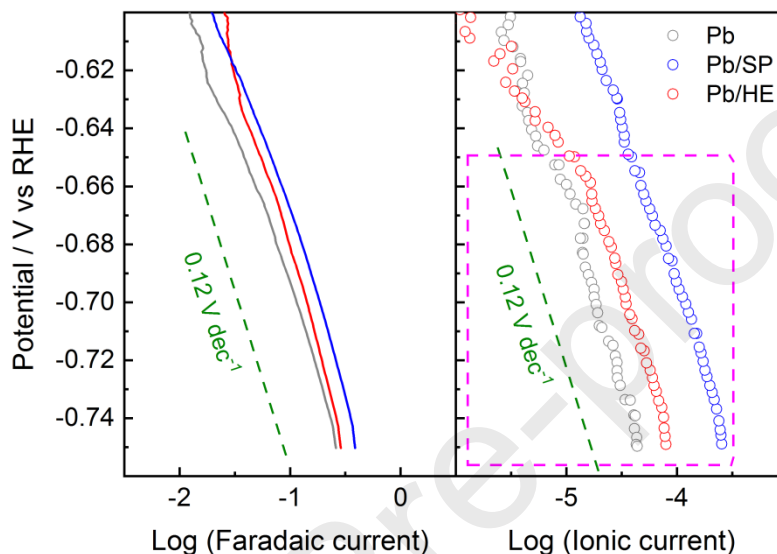
152 **Figure 3.** (A) LSVs and (B) MSLSVs ( $m/z = 2$ ) recorded at Pb (grey line), Pb/SP (blue line) and  
 153 Pb/HE (red line) electrodes.  $V = 1 \text{ mV s}^{-1}$ ;  $5 \text{ M H}_2\text{SO}_4$ .  $T = 25 \text{ }^\circ\text{C}$ .

154

155 Finally, Tafel plots were constructed with the aim of analyzing the reaction mechanism of  
 156 the HER at Pb/SP, Pb/HE and Pb electrodes. **Figure 4** shows Tafel slopes calculated from  
 157 LSV and MSLSV for each sample. Interestingly, both signals (ionic and faradaic currents)  
 158 reveal a Tafel slope of  $0.120 \text{ V dec}^{-1}$  which indicates that the Volmer reaction is the rate-

159 determining step (RDS), as would be expected for *sp* metals [26]. The last implies a similar  
 160 reaction mechanism for the HER at all materials and suggests that the exchange current  
 161 density ( $i_0$ ) is the main parameter affected by the nature of the additive.

162



163

164 **Figure 4.** Tafel plots achieved with faradaic (left panel) and ionic ( $m/z = 2$ , right panel) for Pb (grey),  
 165 Pb/SP (blue) and Pb/HE (red) electrodes. The green lines have a slope of  $120 \text{ mV dec}^{-1}$ .  $V = 1 \text{ mV s}^{-1}$ ;  
 166  $5 \text{ M H}_2\text{SO}_4$ .  $T = 25 \text{ }^\circ\text{C}$ .

167

#### 168 4- Conclusion

169 A novel electrochemical mass spectrometry was developed and applied to follow the  
 170 hydrogen evolution reaction (HER) in situ at technical negative active materials (NAMs)  
 171 employed in lead–acid batteries (LABs). Using this approach, accurate onset potentials and  
 172 reaction mechanisms for the HER at NAM electrodes were determined for the first time. The  
 173 novel DEMS set-up appears to be a valuable technique for studying the HER at NAM  
 174 electrodes in operando during the charging process of LABs.

175

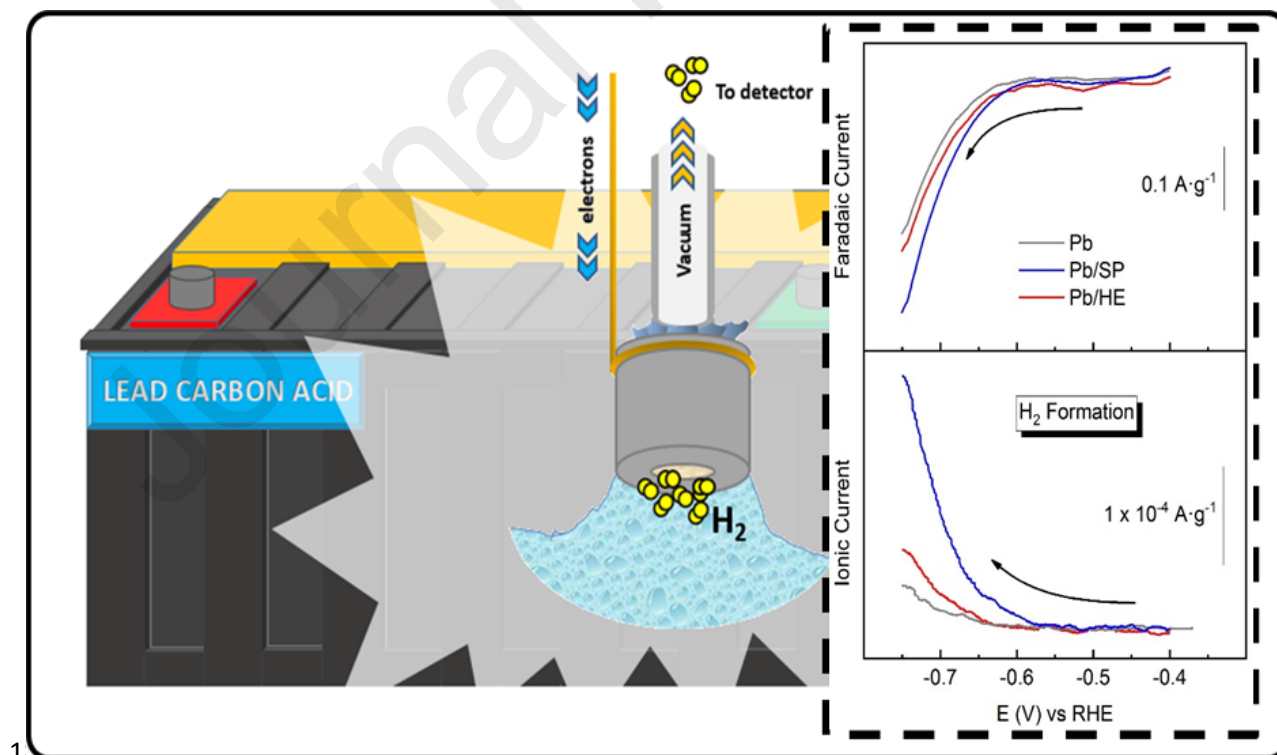
176 **ACKNOWLEDGMENTS**

177 The authors acknowledge financial support of this work by grants from MINCyT-Córdoba  
 178 (PIODO 2018) and Secretaría de Ciencia y Técnica (SECyT), UNRC (PPI) Argentina. F.F,  
 179 and G.A.P. are permanent research staff of CONICET. T.M.M. thanks Pla-Ka S.A. and  
 180 CONICET for doctoral scholarships. In addition, this work has been supported by the  
 181 Ministerio de Ciencia e Innovación (MCIN) under projects PCI2020-112249 and PID2020-  
 182 117586RB-I00 funded by MCIN/AEI/10.13039/501100011033, and by the Canarian Agency  
 183 for Research, Innovation and Information Society (ACIISI, ProID2021010098). G.G.  
 184 acknowledges NANOTec, INTech, Cabildo de Tenerife and ULL for laboratory facilities.

185 **APPENDIX A. SUPPLEMENTARY DATA**

186 Supplementary data to this article can be found online at \*\*\*.

187

188 **REFERENCES**

190

191 **Highlights**

- 192 • DEMS is employed to study a lead/carbon anode for use in a lead–acid battery (LAB)
- 193 • A new DEMS setup makes it possible to follow the HER at the Pb/carbon anode.
- 194 • Independent measurement of HER expands the study of reaction mechanisms in LABs

195

196

197

**CRedit author statement**

198

199 Conceptualization, G.G., G.A.P., E.P. and F.F.; methodology, T.M.M.; validation, G.G.,  
200 G.A.P., E.P. and F.F.; formal analysis, G.G. and G.A.P.; data curation, T.M.M.; writing—  
201 original draft preparation, G.G. and G.A.P.; writing—review and editing, G.G. and G.A.P.;  
202 funding acquisition, G.G., G.A.P., E.P. and F.F. All authors have read and agreed to the  
203 published version of the manuscript.

204

205

206 **Declaration of interests**

207

208  The authors declare that they have no known competing financial interests or personal  
209 relationships that could have appeared to influence the work reported in this paper.

210

211  The authors declare the following financial interests/personal relationships which may be  
212 considered as potential competing interests:

213

214

215

216

217

218

- 
- [1] S.P. Thompson, Recherches sur l'Électricité, *Nature* 21 (1879) 150.
- [2] P. Kurzweil, Gaston Planté and his invention of the lead–acid battery—The genesis of the first practical rechargeable battery, *J. Power Sources* 195 (2010) 4424-4434. <https://doi.org/10.1016/j.jpowsour.2009.12.126>
- [3] P.T. Moseley, D.A.J. Rand, A. Davidson, B. Monahov, Understanding the functions of carbon in the negative active-mass of the lead–acid battery: A review of progress, *J. Energy Storage* 19 (2018) 272-290. <https://doi.org/10.1016/j.est.2018.08.003>
- [4] R. Marom, B. Ziv, A. Banerjee, B. Cahana, S. Luski, D. Aurbach, Enhanced performance of starter lighting ignition type lead-acid batteries with carbon nanotubes as an additive to the active mass, *J. Power Sources* 296 (2015) 78-85. <https://doi.org/10.1016/j.jpowsour.2015.07.007>
- [5] H. Yang, Y. Qiu, X. Guo, Lead oxide/carbon black composites prepared with a new pyrolysis-pickling method and their effects on the high-rate partial-state-of-charge performance of lead-acid batteries, *Electrochim. Acta* 235 (2017) 409-421. <https://doi.org/10.1016/j.electacta.2017.03.138>
- [6] H.Y. Hu, N. Xie, C. Wang, F. Wu, M. Pan, H.F. Li, P. Wu, X.D. Wang, Z. Zeng, S. Deng, M.H. Wu, K. Vinodgopal, G.P. Dai, Enhancing the performance of motive power lead-acid batteries by high surface area carbon black additives, *Appl. Sci.* 9 (2019) 186. <https://doi.org/10.3390/app9010186>
- [7] J. Xiang, C. Hu, L. Chen, D. Zhang, P. Ding, D. Chen, H. Liu, J. Chen, X. Wu, X. Lai, Enhanced performance of Zn(II)-doped lead-acid batteries with electrochemical active carbon in negative mass, *J. Power Sources* 328 (2016) 8-14. <https://dx.doi.org/10.1016/j.jpowsour.2016.07.113>
- [8] D. Pavlov, P. Nikolov, T. Rogachev, Influence of carbons on the structure of the negative active material of lead-acid batteries and on battery performance, *J. Power Sources* 196 (2011) 5155-5167. <https://doi.org/10.1016/j.jpowsour.2011.02.014>
- [9] M. Blecua, E. Fatas, P. Ocon, J. Valenciano, F. de la Fuente, F. Trinidad, Influences of carbon materials and lignosulfonates in the negative active material of lead-acid batteries for microhybrid vehicles, *J. Energy Storage* 11 (2017) 55-63. <https://doi.org/10.1016/j.est.2017.01.005>
- [10] L.T. Lam, R. Louey, Development of ultra-battery for hybrid-electric vehicle applications, *J. Power Sources* 158 (2006) 1140-1148. <https://doi.org/10.1016/j.jpowsour.2006.03.022>

- [11] L. Wang, W. Zhang, L. Gu, Y. Gong, G. Cao, H. Zhao, Y. Yang, H. Zhang. Tracking the morphology evolution of nano-lead electrodeposits on the internal surface of porous carbon and its influence on lead-carbon batteries, *Electrochim. Acta* 222 (2016) 376-384. <https://doi.org/10.1016/j.electacta.2016.10.189>
- [12] P.T. Moseley, D.A.J. Rand, K. Peters, Enhancing the performance of lead-acid batteries with carbon – In pursuit of an understanding, *J. Power Sources* 295 (2015) 268-274 <https://doi.org/10.1016/j.jpowsour.2015.07.009>
- [13] M.A. Deyab, Effect of halides ions on H<sub>2</sub> production during aluminum corrosion in formic acid and using some inorganic inhibitors to control hydrogen evolution, *J. Power Sources* 242 (2013) 86-90. <https://doi.org/10.1016/j.jpowsour.2013.05.066>
- [14] Y.M. Wu, W.S. Li, X.M. Long, F.H. Wu, H.Y. Chen, J.H. Yan, C.R. Zhang, Effect of bismuth on hydrogen evolution reaction on lead in sulfuric acid solution, *J. Power Sources* 144 (2005) 338-345. <https://doi.org/10.1016/j.jpowsour.2004.10.019>
- [15] K. Jo, E. Hwang, A quantitative evaluation of oxygen reduction and hydrogen evolution reaction contributions to Pb corrosion, *J. Electroanal. Chem.* 850 (2019) 113393. <https://doi.org/10.1016/j.jelechem.2019.113393>
- [16] S. Kang, M. Shang, M.A. Spence, M. Andrew, S. Liu, J. Niua, Dynamic charge acceptance and hydrogen evolution of a new MXene additive in advanced lead-acid batteries via a rapid screening three-electrode method, *Chem. Commun.* 54 (2018) 3456-3459. <https://doi.org/10.1039/C8CC00086G>
- [17] S. Zhang, H. Zhang, W. Xue, J. Cheng, W. Zhang, G. Cao, H. Zhao, Y. Yang, A layered-carbon/PbSO<sub>4</sub> composite as a new additive for negative active material of lead-acid batteries, *Electrochim. Acta* 290 (2018) 46-54. <https://doi.org/10.1016/j.electacta.2018.08.090>
- [18] F. Wang, C. Hu, M. Zhou, K. Wang, J. Lian, J. Yan, S. Cheng, K. Jiang, Research progresses of cathodic hydrogen evolution in advanced lead-acid batteries, *Sci. Bull.* 61 (2016) 451-458. <https://doi.org/10.1007/s11434-016-1023-0>
- [19] S. Pérez-Rodríguez, G. García, M.J. Lázaro, E. Pastor, DEMS strategy for the determination of the difference in surface acidity of carbon materials, *Electrochem. Commun.* 90 (2018) 87-90. <https://doi.org/10.1016/j.elecom.2018.04.014>
- [20] S. Díaz-Coello, G. García, M.C. Arévalo, E. Pastor, Precise determination of Tafel slopes by DEMS. Hydrogen evolution on tungsten-based catalysts in alkaline solution, *Int. J. Hydrogen Energy* 44 (2019) 12576-12582. <https://doi.org/10.1016/j.ijhydene.2019.02.151>
- [21] G. García, M. Roca-Ayats, O. Guillén-Villafuerte, J.L. Rodríguez, M.C. Arévalo, E. Pastor, Electrochemical performance of  $\alpha$ -Mo<sub>2</sub>C as catalyst for the hydrogen evolution reaction, *J. Electroanal. Chem.* 793 (2017) 235-241. <https://doi.org/10.1016/j.jelechem.2017.01.038>

- [22] R. Ianniello, V.M. Schmidt, A simplified DEMS set up for electrocatalytic studies of porous PtRu alloys, *Ber. Bunsenges. Phys. Chem.* 99 (1995) 83-86. <https://doi.org/10.1002/bbpc.19950990114>
- [23] C. Niether, M.S. Rau, C. Cremers, D.J. Jones, K. Pinkwart, J. Tübke, Development of a novel experimental DEMS set-up for electrocatalyst characterization under working conditions of high temperature polymer electrolyte fuel cells, *J. Electroanal. Chem.* 747 (2015) 97-103. <https://doi.org/10.1016/j.jelechem.2015.04.002>
- [24] M. Heinen, Y.X. Chen, Z. Jusys, R.J. Behm, In situ ATR-FTIRS coupled with on-line DEMS under controlled mass transport conditions—A novel tool for electrocatalytic reaction studies, *Electrochim. Acta* 52 (2007) 5634-5643. <https://doi.org/10.1016/j.electacta.2007.01.055>
- [25] D. Pavlov, *Lead-Acid Batteries: Science and Technology. A Handbook of Lead-Acid Battery Technology and Its Influence on the Product*, second ed., Elsevier, 2017. ISBN 978-0-444-59552-2.
- [26] G. Zhao, W. Sun, Electrochemical hydrogen evolution reaction. In: J. Ma (Ed.), *Photo- and Electro-Catalytic Processes*, Wiley, 2022, Chapter 3. <https://doi.org/10.1002/9783527830084.ch3>